Asian Journal of Nanoscience and Materials 4 (2021) 53-66

Asian Journal of Nanoscience and Materials

Journal homepage: www.ajnanomat.com

Orginal Research Article

Effects of fluorodeoxyglucose magnetic nanoparticles on NCI-H727 and SH-SY5Y cancer cells

Perihan Unak[a,*], Rumbidzai Cheryl Budiyo[b], Alex Horsnzky[b], Volkan Yasakci[a], Gillian Pearce[c], Steve Russell[b], Omer Aras[d], Oguz Akin[d], Julian Wong[e]

[a] *Ege University, Institute of Nuclear Sciences, Department of Nuclear Applications, Bornova Izmir, 35100, Turkey*

[b] *Aston University, School of Life and Health Sciences, Aston Triangle, Birmingham, B4 7ET, United Kingdom*

[c] *School of Engineering and Applied Sciences, Aston University, Aston Triangle, Birmingham, B4 7ET, United Kingdom*

[d] *Memorial Sloan Kettering Cancer Centre, Department of Radiology, New York, USA*

[e] *University Hospital Singapore, Cardiothoracic and Vascular Surgery Department, Singapore*

ARTICLE INFORMATION

Received: 9 October 2020
Received in revised: 7 November 2020
Accepted: 24 November 2020
Available online: 19 December 2020

DOI: 10.26655/AJNANOMAT.2021.1.5

KEYWORDS

Magnetic nanoparticles
Fluorodeoxyglucose
SH-SY5Y
NCI-H727
Spheroids

ABSTRACT

We present a report regarding the cytotoxic effects of iron-based magnetic nanoparticles conjugated with fluorodeoxyglucose (FDG-mNPs) on the viability of NCI-H727 and SH-SY5Y cancer cells. MTT assays were performed to determine cell viability in treated cancer cells grown under standard 2D culture conditions. FDG-mNP concentrations of 0.075 mg/mL, 0.15 mg/mL, and 0.3 mg/mL decreased mean cell viability of NCI-H727 cells to 92.5%, 82.9%, and 75% respectively. FDG-mNPs was also shown to have a detrimental effect on the viability of SY5Y cells: a decrease of 5.7%, 18.6%, and 36.4% was found for SY5Y cells treated with 0.075 mg/mL, 0.15 mg/mL, and 0.3 mg/mL concentrations of FDG-mNPs, respectively. When NCI-H727 and SH-SY5Y cancer cells were grown as 3D spheroids, morphology was visibly changed and the number of viable cells was decerased in spheroids treated with FDG-mNPs compared with untreated spheroids. The results of our study demonstrated that FDG-mNP has toxic effects on NCI-H7272 and SY5Y cancer cells, and we conclude that conjugated FDG-mNPs are promising in the development of clinical applications for the destruction of cancer cells.

Corresponding author, email: perihan.unak@gmail.com (P. Unak).
Tel.: +90 5365131806.

Graphical Abstract

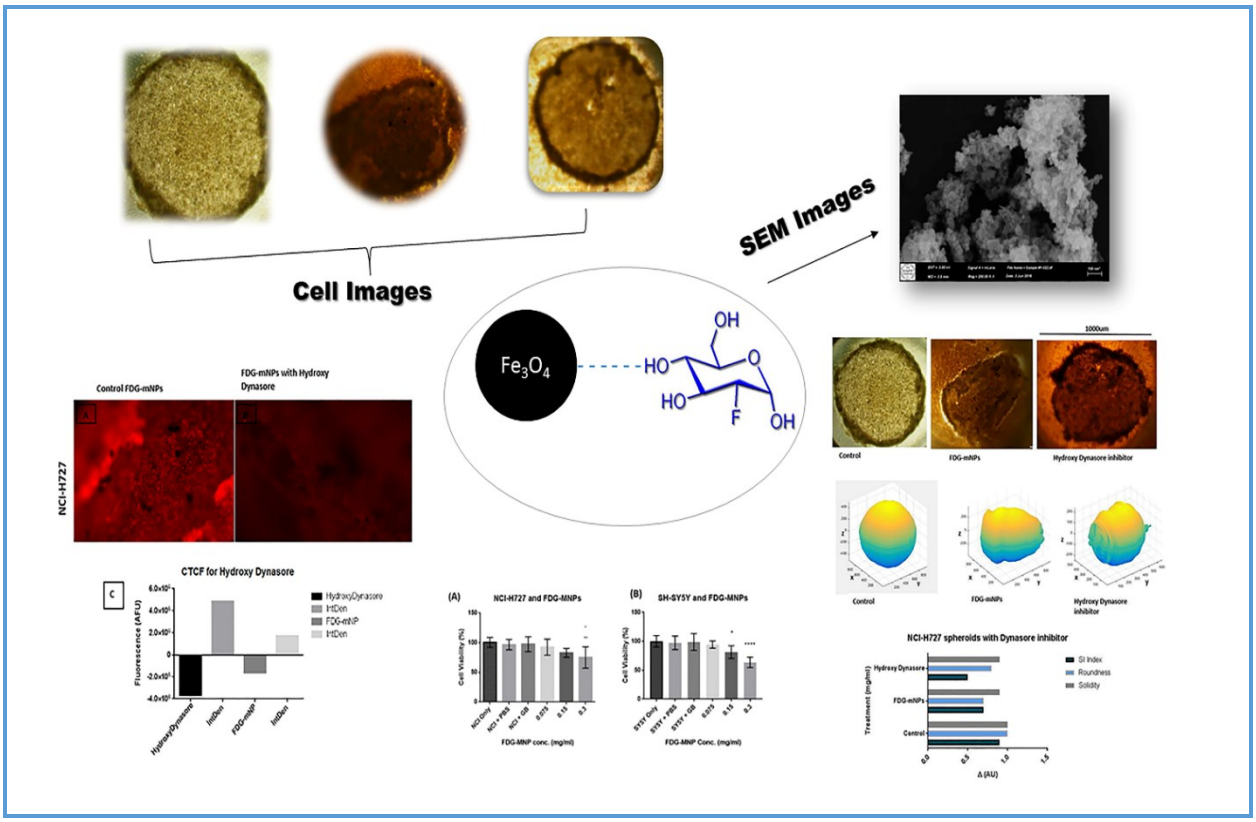

Introduction

Nanoparticles typically have a dimension of ≤100 nm. They can be made from a range of materials including biological materials (viral), lipids, polymers, and inorganic materials (metal and quantum dots) [1]. Nanoparticles can be modified to deliver anti-cancer drugs and to be used as imaging probes. Nanoparticles have an enormous impact in the field of medical science, particularly for drug screening and drug delivery.

Drug delivery with nanoparticles first reached a phase I clinical trial in 1985, and the first nanoparticles involving doxorubicin reached the pharmaceutical market in the mid-1990s [2]. Since then, at least ten nanomedicines have been approved by the United States Food and Drug Administration [3]. One of the main reasons they are an attractive avenue for drug delivery is that they have a large functional surface that is capable of binding, absorbing, and carrying other particles including drugs [4]. For cancer therapy, the use of nanoparticles leads to improved drug solubility and decreased systemic toxicity in comparison with chemotherapy [5]. Nanoparticles can also evade the immune system due to their size [6]. Recently, fluorodeoxyglucose-conjugated magnetic nanoparticles (FDG-mNPs) have been shown to be effective in the targeting of neuroblastomas [7]. The conjugation of mNPs with the glucose analogue fluorodeoxyglucose (FDG) is thought to improve mNP cellular "incorporation and cytotoxicity in cancer cell lines. It is well known that cancer cells have a great affinity for glucose uptake due to the Warburg effect [8, 9], and FDG is a glucose analogue that is rapidly taken up by cancer cells [7, 10]. Meanwhile, metal and

magnetic nanoparticles themselves induce apoptosis in cancer cells. For drug screening, the surface of nanoparticles can be changed (e.g. crosslinked with glucose or antibodies) to efficiently target cancer sites [11]. To study if FDG-mNPs successfully enter cancer cells via endocytosis, the Hydroxy Dynasore inhibitor which inhibits clathrin-mediated endocytosis can be used [12]. Additionally, as 2D cell cultures have been shown not to represent the native environment of tumors, 3D cell culture can be utilized alongside a 2D cell culture for a more robust analysis. 3D cell cultures have similar gradients to tumors which make them excellent candidates for drug screening [13]. The objective of the present study was to determine whether FDG-mNPs can exert cytotoxic effects on NCI-H727 and SH-SY5Y cancer cells.

Experimental

The reagents used were purchased at the highest purity available as described below. $FeCl_3$, (3-aminopropyl) triethoxysilane (APTES), cysteamine, tetraethyl orthosilicate (TEOS), Dowex 50 cation exchange resin, Amberlite anion exchange resin, C18 pre-cartridge, cellulose coated TLC sheets, and MTT (3-[4,5-dimethylthiazol-2-yl]-2,5-diphenyltetrazoliumbromide) were purchased from Sigma-Aldrich (Missouri, USA). Na_2SO_3, dimethylformamide, N-hydroxysuccinimide, Kryptofix, NaF, NH_3 were obtained from Merck (Darmstadt, Germany). Mannose triflate, K_2CO_3, and Ambersep 900 quaternary ammonium anion exchange resin were obtained from Fluka (Buchs, Switzerland). Fasentin and Hydroxy Dynasore were obtained from TOCRIS Bioscience (Abingdon, UK). Propidium iodide was purchased from Invitrogen Thermofisher Scientific (Waltham, MA, USA). The human lung non-small cell carcinoma cell line NCI-H727 was obtained from the European Collection of Authenticated Cell Cultures (ECACC94060303). The human neuroblastoma cell line SH-SY5Y was obtained from the European Collection of Authenticated Cell Culture (ECACC94030304) from a 4-year old child with neuroblastoma. The following equipment was used for experimental processes: a dynamic light scattering device (Malvern Nano ZS DLS, Malvern, UK), a scanning electron microscope (SEM) (Thermo Fisher Scientific QUANTA 250, FEG, Massachusetts, USA), a plate reader (Biotek, Elx800 Universal Absorbance Microplate Reader, USA), a widefield microscope (Leica Microsystems, Germany), a haemocytometer (Carl Zeiss, Jena Germany), and an EVOS XL imaging system (Thermofisher, UK).

Synthesis and characterization of FDG-mNPs

MNPs were synthesized, silica-coated, and fabricated with tetraethyl orthosilicate (TEOS). The modified mNPs were conjugated with non-radiactive F using NaF. mNPs and FDG-mNPs characterized similarly as described in our previous reports [10, 14, 15, 16]. Briefly, the hydrodynamic diameter of mNPs or FDG-mNPs was measured using DLS. For this, mNPs or FDG-mNPs were dispersed in 20% dextrose solution at a concentration of 100 μg mL^{-1} and then measured at 25 °C. Measurements were repeated three times, and the results were expressed as the mean ± standard deviation. Particle size and morphology of the synthesized mNPs and FDG-mNPs were obtained using SEM.

In vitro studies

Cell lines

The cell lines were cultured at Roswell Park Memorial Institute 1640 (RPMI, Sigma- Aldrich, USA) and were supplemented with 1% (v/v) L-Glutamine, 1% (v/v) Penicillin-Streptomycin. An additional 10% (v/v) heat inactivated foetal

bovine serum was added to the media. The cells were cultured in 75 cm^3 T-flasks. The flasks were incubated under normal conditions (37 °C, 5% CO_2, and 95% humidity). Before reaching confluence, the cell media was changed every 2 days. Cells were passaged when they reached 80%–90% confluence with 2.5 mL trypsin-EDTA (Sigma-Aldrich, USA) for 5–8 minutes. The actions of trypsin-EDTA were inhibited by using 2.5 mL of RPMI-1640 media. The NCI-H727 cells were centrifuged at 700 g and the SH-SY5Y cells were centrifuged at 1000 g for 5 min in order to obtain a pellet of cells for each of these cell lines. Each pellet of cells was re-suspended in 5 mL media. The number of cells in suspension for the NCI-H7272 cell line was determined using a haemocytometer with the aid of a microscope (Zeiss model) and a manual counter.

MTT assay

In order to investigate the effects of FDG-mNPs on the viability of NCI-H727 and SH-SY5Y cells, both cell lines (NCI-H727 and SH-SY5Y) were seeded separately into 96-well plates at 35,000 cells per well. Once seeded, the plates were incubated under normal cell culture conditions (37 °C, 5% CO_2, and 95% humidity) for 24 h to ensure that the cells adhere to the wells before FDG-mNP treatment. FDG-mNPs were pipetted into each well at a volume of 0.075 mg/mL, 0.15 mg/mL, or 0.3 mg/mL. Glass beads and/or phosphate buffered saline (PBS) in 200 µL RPMI media were also introduced into a portion of the wells. The 96-well plates were incubated under normal cell culture conditions (37 °C, 5% CO_2, and 95% humidity) for an additional period of 24 h. After the 24 h incubation period, the 96-well plates were washed with PBS. Subsequently, 200 µL of RPMI media was added to each well followed by 10 µL of MTT solution dissolved in 5 mg/mL of PBS, and then the 96-well plates were further incubated for 4 h under normal cell culture conditions (37 °C, 5% CO_2, and 95% humidity). After incubation, absorbance was read at 590 nm using the Biotek plate reader.

The same procedure was used for 1 µM, 0.5 µM, 0.25 µM, and 0.125 µM FDG-mNP concentrations and PBS and cell-only wells. Absorbance values were converted into percentages in Excel using equation (1) for *viability%*.

$$Viability\% = \frac{Absorbance\ of\ Treated}{Control\ Cells} x10 \qquad (1)$$

Spheroid generation

Corning plates (Corning®, USA) were used to seed 20,000 cells from the NCI-H727 and HTR-8 cell lines. RPMI media supplemented with 5% FBS, 1% Penicillin/Streptomycin, and 1% L-Glutamine were used to ensure a final volume of 100 µL. The Corning plates were incubated under normal cell culture conditions (37 °C, 5% CO_2, and 95% humidity) for 24 h to permit formation of spheroids between 200 and 500 µm in size. This was determined using Feret's diameter function found in ImageJ.

Morphological evaluation of untreated spheroids

To determine whether treated spheroids have reduced cell viability, first, NCI-H727 spheroids with appropriate morphology were first selected. Spheroid images of spheroids before any treatment were obtained using the EVOS XL imaging system. The free hand toold within the Fiji open-source image processing package [17] which consists of the ImageJ software with several extra plugins was used produce binary masks of the spheroid images. The EVOS XL images were also imported to Reconstruction and Visualisation from a Single Projection (ReVISP), an open-source software [18] that enables the visualization of the 3D projection of spheroids. ReVISP was used to

reconstruct the three-dimensional shape of spheroids. The reconstructed images were also imported into ImageJ software [19] and, with Macro S1 [20, 21], three morphological quantitative parameters were assessed: solidity, roundness, and sphericity. The solidity parameter was assessed using the ImageJ "solidity" function which measures the surface regularity of spheroids; if spheroids had values between 0.90–1, they were considered to have a regular rather than irregular surface [22]. The roundness parameter was assessed using the ImageJ "roundness" function which measures how close the spheroid image is to a circle. The sphericity parameter was assessed using the ImageJ "circularity" function which measures the spheroid's closeness to a spherical geometry shape in accordance with equations (2) and (3) [19]:

$$Circularity = \frac{4rr\ x\ Area}{Perimeter^{\ 2}} \quad (2)$$

$$Sphericity\ Index = \boldsymbol{j} Circularity \quad (3)$$

According to Zanoni et al, SI values can be categorised as spherical (SI≥0.90) or non-spherical (SI<0.90) [23]. Spheroids selected for treatment with FDG-mNPs were those that were determined to be spherical (SI>0.90).

Treatment of spheroids with FDG-mNP with or without hydroxy dynasore

In order to examine whether FDG-mNP treated cells are transported into cancer cells via endocytosis, selected NCI-H727 spheroids were treated with Hydroxy Dynasore, an endocytosis inhibitor. Hydroxy Dynasore was solubilized in DMSO to create a 5 mM stock solution. The NCI-H727 spheroids were treated with Hydroxy Dynasore and incubated for 1 h under normal cell culture conditions (37 °C, 5% CO_2, and 95% humidity). After 1 h, the spheroids were subjected to a concentration of 0.3 mg/mL of FDG-mNPs and incubated for a further 1 h under normal cell culture conditions. Following the additional incubation period, the spheroids were imaged with the EVOS XL imaging system and fixed with 1X fixative solution.

Treatment of Spheroids with FDG-mNP with or without fasentin

Additionally, in order to examine whether FDG-MNP treated cells are transported into cancer cells via GLUT-1 transporters, selected NCI-H727 spheroids were treated with fasentin, a GLUT-1 inhibitor. Fasentin was solubilized in DMSO to create a 10 mM stock solution. NCI-H727 spheroids were treated with fasentin to a final concentration of 5 mM per well and incubated for 1 h under standard cell culture conditions (37 °C, 5% CO_2, and 95% humidity). After 1 h, the spheroids were treated with FDG-MNPs at a concentration of 0.3 mg/mL and incubated for a further 1 h under normal cell culture conditions. Finally, the spheroids were imaged with the EVOS XL imaging system and fixed using 1X fixative solution.

Staining and image analysis of treated spheroids

Propidium iodide is a stain that penetrates the nucleus of dead cells to produce a red colour at 493 nm. Prior to staining with propridium iodide, treated spheroids were washed with PBS. Thereafter, they were stained for 10 min. Images were obtained using the Widefield microscope, with red fluorescence observed in dead cells within the spheroids. Images were acquired using the Widefield microscope for untreated spheroids, FDG-mNPs treated spheroids, and FDG-mNP plus Hydroxy Dynasore treated spheroids. Subsequently, in ImageJ software, the corrected total cell fluorescence (CTCF) was calculated using the formula Area×Intensity Density−Background to

determine the number of viable cells and the resulting data was imported into a Microsoft Excel workbook.

Statistical analysis

Statistical analysis was carried out using Prism software (GraphPad, Inc., La Jolla, California, USA). Statistical analyses included one-way and two-ANOVA alongside post hoc Tukey's Test.

Results and Discussion

Structural properties of mNPs and FDG-mNPs

According to DLS measurement, the nanoparticles were homogeneously dispersed in dextrose (80% water, 20% dextrose) solution and had a medium size of 176.7±4.7 nm (n=5) together with their hydrodynamic radius. The surface potential of mNPs and FDG-mNPs was measured to be −4.77±0.918 mV and 21.26±0.862 mV, respectively. The increased surface potential of FDG-mNPs at the physiologically relevant pH 7.4 suggests good colloidal stability of FDG mNPs.

SEM images showed that FDG-mNPs had a mean size of 10–20 nm and a cubic spinel structure (Figure 1). Meanwhile, mNPs possessed a particle shape that was a uniform homogeneous cubic crystal structure, with a particle size of around 20–30 nm.

Overall, the structural properties of synthesized mNPs and FDG-mNPs are in line with findings from previous studies [7, 14, 15, 16].

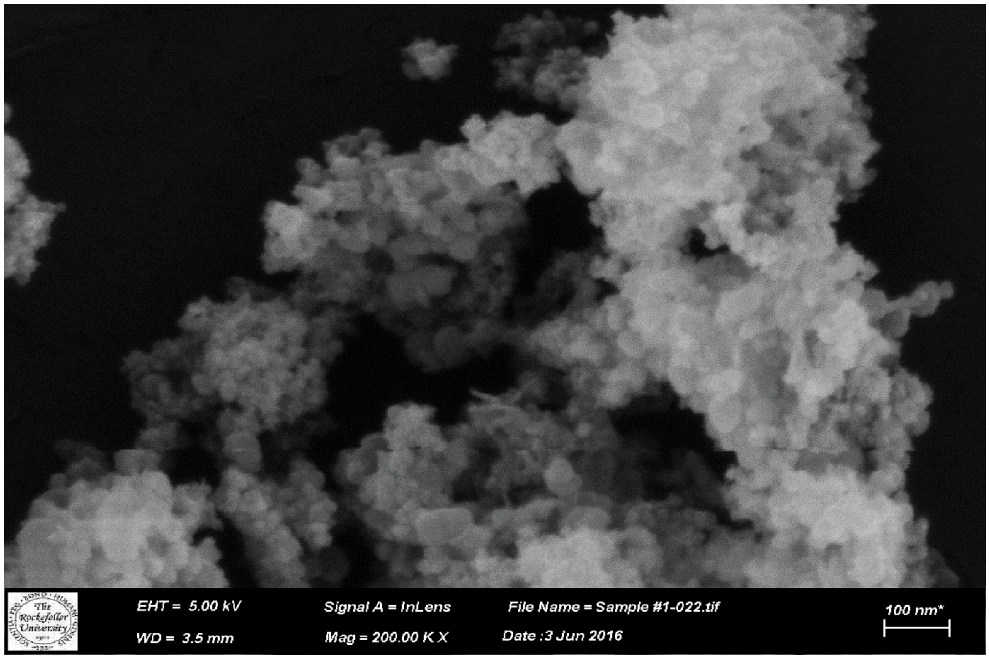

Figure 1. SEM image of FDG-mNPs

Cell viability of FDG-mNP treated NCI-H727 and SH-SY5Y cells grown in 2D culture

Exposure of NCI-H727 and SH-SY5Y cells to FDG-mNP at 0.075 mg/mL, 0.15 mg/mL, and 0.3 mg/mL concentrations led to decreased mean cell viability in both cell lines (Figure 2). As expected, higher FDG-mNP concentrations led to higher decreases in mean cell viability for both cell lines (e.g., by 5.7%, 18.6%, and 36.4%, for SH-SY5Y cells exposed to 0.075 mg/mL,15

mg/mL, and 0.3 mg/mL FDG-mNPs, rsepectively). Mean cell viability of NCI-H727 cells+0.3 mg/mL FDG-mNPs was significantly different compared with that of NCI-H727 cells+glass beads+0.3 mg/mL FDG-mNPs ($p < 0.01$) or NCI-H727+PBS+0.3 mg/mL FDG-mNPs ($p<0.05$). Mean cell viability of SH-SY5Y cells+0.3 mg/mL was also significantly different when compared with that of SH-SY5Y+glass beads and 0.3 mg/mL ($p<0.0001$) and SH-SY5Y +PBS+0.3 mg/mL FDG-mNPs. At lower FDG-mNP concentrations, mean cell viability of SH-SY5Y cells+0.15 mg/mL FDG-mNPs was significantly different when compared with SH-SY5Y+glass beads+0.15 mg/mL FDG-mNPs and, and SH-SY5Y+PBS+0.15 mg/mL FDG-mNPs and ($p<0.05$).

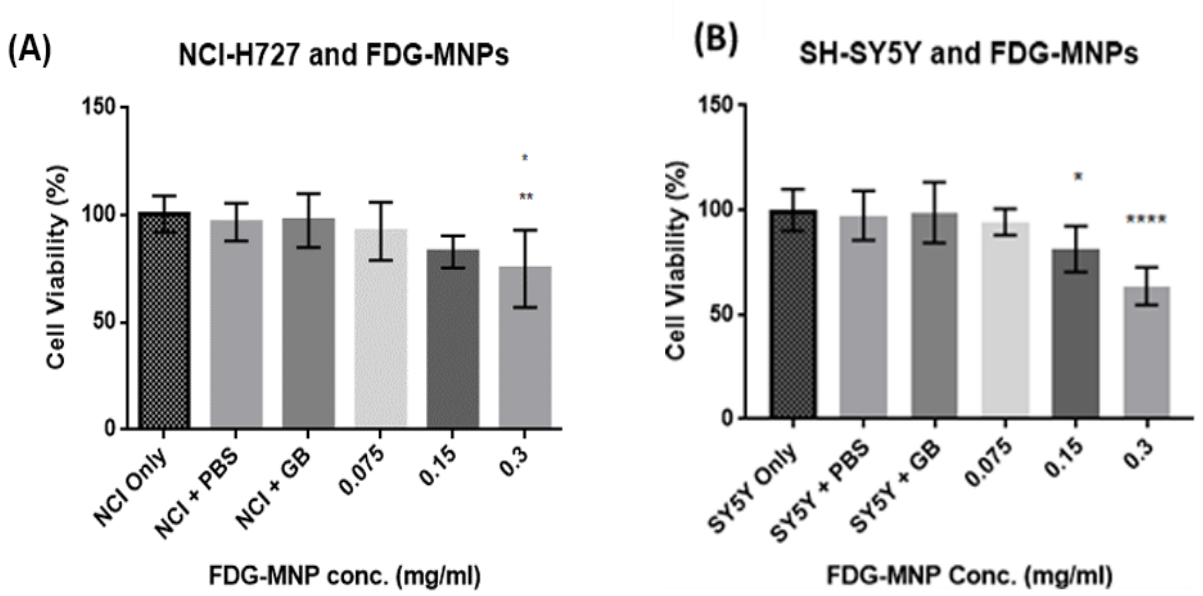

Figure 2. Cell viability percentages of NCI-H727 and SH-SY5Y cells after treatment with FDG-mNPs**.** Charts displaying cell survival percentages of NCI-H727 and SH-SY5Y cells treated with increasing concentrations of FDG-mNPs (0.075 mg/mL, 0.15 mg/mL, 0.3 mg/mL). Where bars are labeled as "NCI/SY5Y only," samples contained NCI/SY5Y and RPMI-1640. Bars labeled as "NCI/SY5Y+PBS" represent samples that contained cells and PBS only. Samples labeled as "NCI/SY5Y+ GB" represent samples containing cells, PBS, and glass beads (1% w/v). Data expressed represent mean values±SD from independent experiments performed in triplicate (n=3). **** $p<0.0001$, ** $p<0.01$, * $p<0.05$; one-way ANOVA with correction using Tukey's Test

Morphology and cell viability of FDG-mNP and hydroxy dynasore treated NCI-H727 spheroids

As shown in Figure 3, as seen on images obtained with the EVOS XL microscope, morphology was visibly changed in the spheroid when treated with FDG-mNPs only and when treated with both FDG-mNPs and Hydroxy Dynasore, compared with the untreated spheroid. When quantitative morphological parameters were assessed, roundness and SI were decreased in the spheroid when treated with FDG-mNPs only (roundness=0.7, SI=0.7) and when treated with both FDG-mNPs and Hydroxy Dynasore (roundness=0.8, SI=0.5), compared with the untreated spheroid (roundness=1.0, SI=0.9). Whie solidity decreased slightly, all spheroids,

whether treated or untreated, were found to have a regular spheroid surface (solidty=0.90–1). There was not enough data to detect significant differences in quantitative parameters using two-way ANOVA.

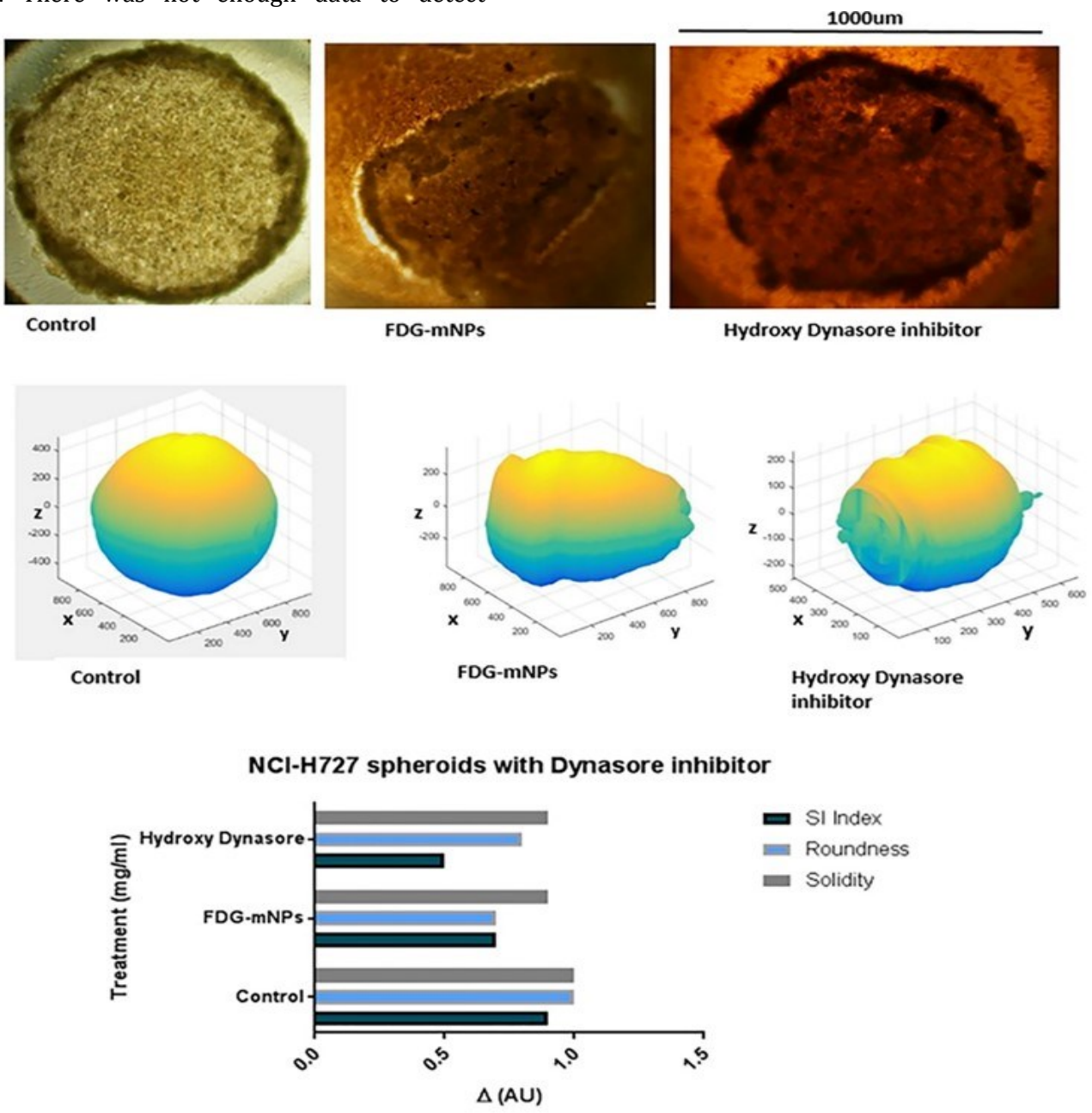

Figure 3. Analysis of morphological changes to NCI-H727 spheroids after FDG-mNP treatment and Hydroxy Dynasore treatment. A) Spheroids with an appropriate sphericity index (SI) were selected and treated with FDG-mNPs, with or without Hydroxy Dynasore 24 hours prior to FDG-mNP treatment, and an EVOS XL microscope was used to obtain images. B) Spheroids were reconstructed using the ReVISP software (https://sourceforge.net/projects/revisp/). C) Quantitative morphological information of the spheroids, including sphericity index (SI), roundness, and solidity. ImageJ software (https://imagej.net/) was used along with Macro S1 for the calculation of

morphological parameters. Samples labeled as "control" received no treatment, samples labeled as "FDG-MNPs" were treated with FDG-mNPs only, and samples labeled as "Hydroxy Dynasore" were treated with Hydroxy Dynasore prior to FDG-mNP treatment

When evaluating cell viability changes in spheroids when treated with FDG-mNPs with or without Hydroxy Dynasore, exposure of NCI-H727 cells to 0.3 mg/mL FDG-mNPs with and without Hydroxy Dynasore decreased CTCF, confirming that there are fewer viable cells for treated cells compared with untreated cells (Figure 4). The reason that CTCF values are negative for both Hydroxy Dynasore and FDG-mNP might be the under-or over-exposure of the fluorescence images.

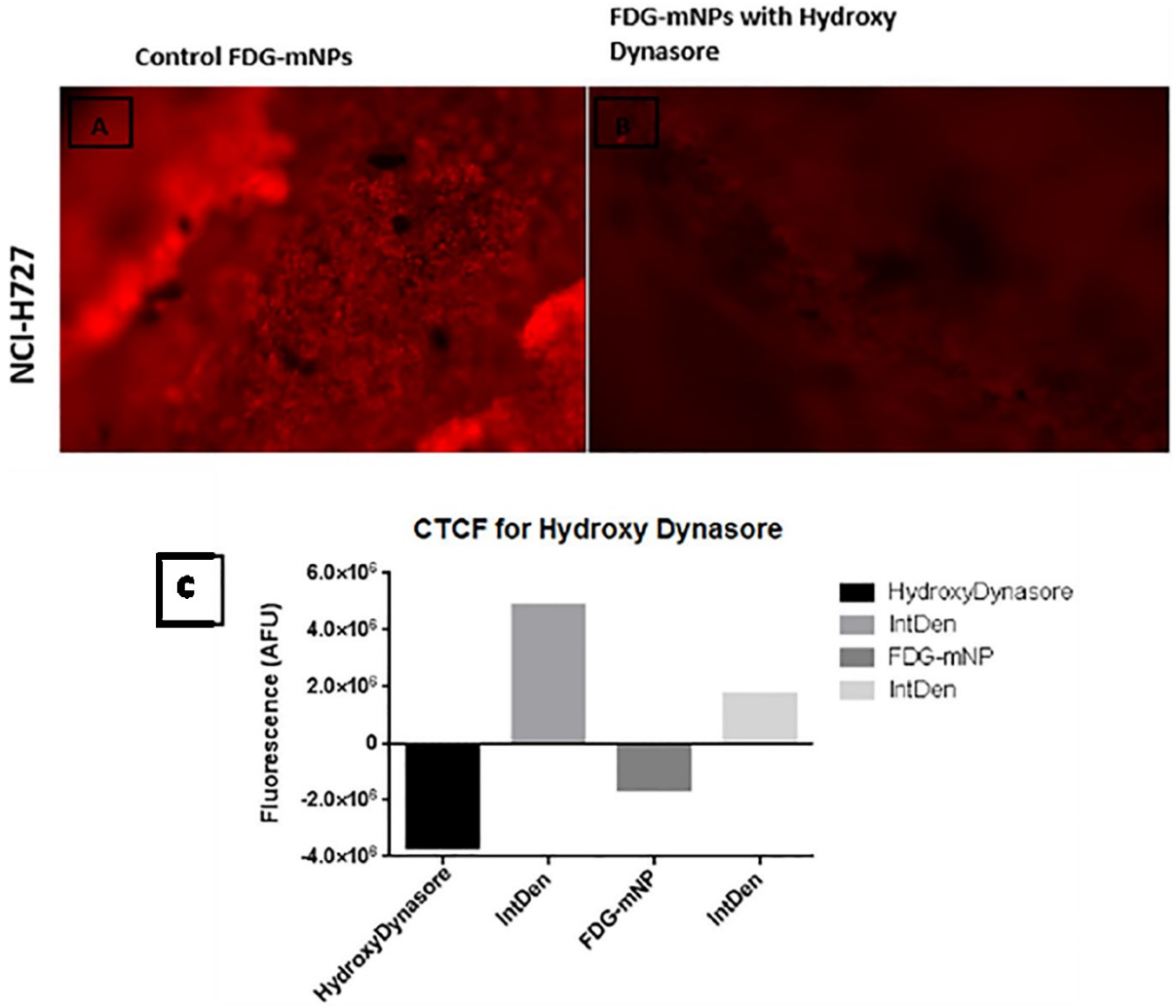

Figure 4. Fluorescence microscopy of NCI-H727 and corrected total cell fluorescence (CTCF). NCI-H727 cells were cultured for 24 hours to allow formation of spheroids and were treated with A) FDG-mNPs only or B) FDG-mNPs and Hydroxy Dynasore. The resulting spheroids were stained with propidium iodide solution (nucleus of dead cells appear red) in 100 mL of media for 10 minutes. Images were acquired using a Widefield microscope at 493 nm. C) CTCF was calculated using the formula Area×Intensity Density–Background using the ImageJ software

Morphology and cell viability of FDG-mNP and fasentin treated spheroids

As shown in Figure 5, as seen on images obtained with the EVOS XL microscope, the spheroid treated with both FDG-mNPs and fasentin showed unchanged morphology compared with the untreated spheroid; however, the spheroid treated with only FDG-mNPs showed changed morphology. When quantitative morphological parameters were assessed, the spheroid treated with only FDG-mNPs showed a larger decrease in SI, roundness, and solidity than the spheroid treated with both fasentin and FDG-mNPs. There was not enough data to detect significant differences in quantitative parameters using two-way ANOVA.

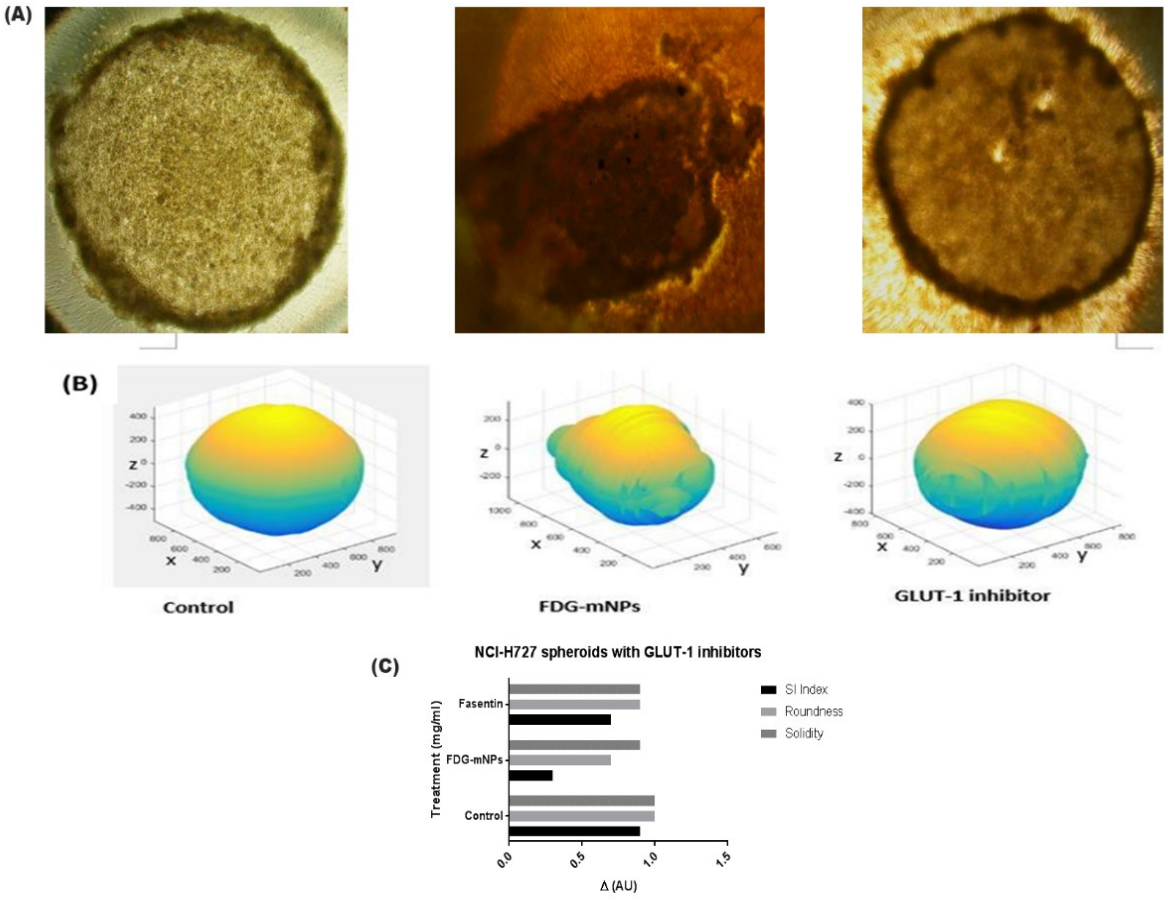

Figure 5. Analysis of morphological changes to NCI-H727 spheroids after treatment with FDG-MNPs and fasentin, a GLUT-1 inhibitor. A) Spheroids with an appropriate sphericity index (SI) were selected and treated with FDG-mNPs, with or without fasentin 24 hours prior to FDG-mNP treatment, and an EVOS XL microscope was used to obtain images. Scale bar 1000 um. B) Spheroids were reconstructed using the ReVISP software (https://sourceforge.net/projects/revisp/). C) Quantitative morphological information of the spheroids, including SI index, roundness, and solidity. ImageJ software (https://imagej.net/) was used along with Macro S1 for the calculation of morphological parameters. Samples labeled as "control" received no treatment, samples labeled as "FDG-MNPs" were treated with FDG-mNPs only, and samples labeled as "fasentin" were treated with fasentin prior to FDG-mNP treatment

When evaluating cell viability changes in spheroids when treated with FDG-mNPs with or without fasentin, exposure of NCI-H727 cells to 0.3 mg/mL FDG-mNPs with and without fasentin decreased CTCF, confirming that there are fewer viable cells for treated cells compared with untreated cells (Figure 6). The reason that CTCF values are negative for both Hydroxy Dynasore and FDG-mNP might be the under- or over-exposure of the fluorescence images.

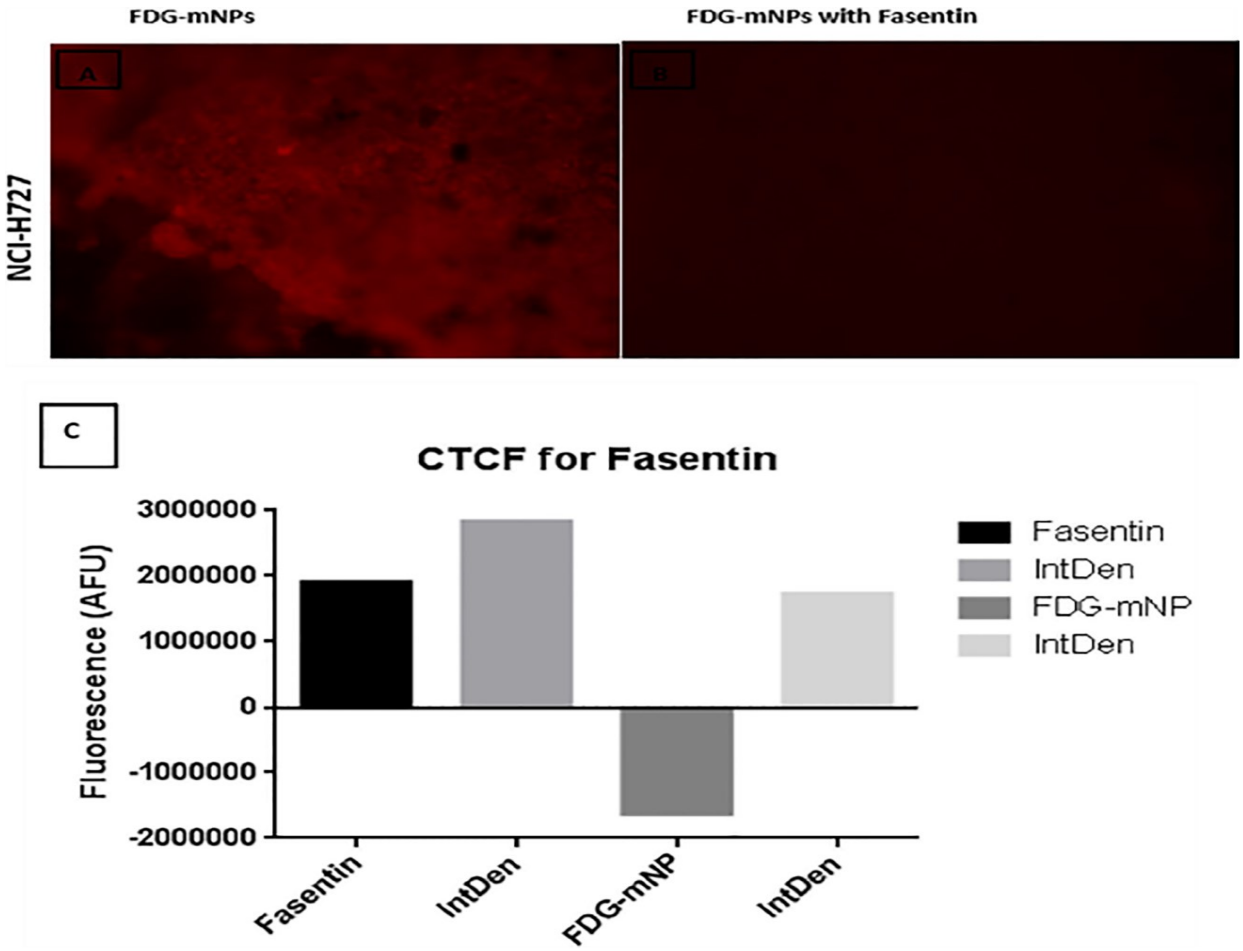

Figure 6. Fluorescence microscopy of NCI-H727 and Corrected Total Cell Fluorescence (CTCF). NCI-H727 cells were cultured for 24 hours to allow formation of spheroids and were treated with A) FDG-mNPs only or B) FDG-mNPs and fasentin. The resulting spheroids were stained with propidium iodide solution (nucleus of dead cells appear red) in 100 mL of media for 10 minutes. Images were acquired using a Widefield microscope at 493 nm. C) CTCF was calculated using Area×Intensity Density−Background taken from using ImageJ software

Advantage of Conjugating FDG with mNPs to Cause Apoptosis in Cancer Cells

Glucose is a vital nutrient in maintaining tumor growth. It mediates signalling that leads to tumor progression. In this study, FDG-mNPs solubilised in PBS decreased cell viability of NCI-H727 and SH-SY5Y cells. This is in line with previous reports of the potential of FDG-mNPs to cause apoptosis in cancer cells. For example, we previously reported [7] that FDG-mNPs mediated neuroblastoma cytotoxicity in conjunction with alternating current magnetic field exposure. In another study, Roa et al.

reported that use of 6-FDG covalently bound to gold nanoparticles caused apoptosis in MCF-7 adenocarcinoma cells and the combination of 6-FDG with radiation increased cell death [24]. Similar to Roa et al, Hu et al found that the use of glucose-coated gold nanoparticles combined with X-ray exposure resulted in a greater targeted cancer destroying effect [25].

Apoptosis is caused by caspases, a group of intracellular cysteine proteases. There are many pathways that have been studied but only a few have been studied extensively. One of these pathways is the tumour necrosis factor (TNF) pathway. TNF receptors trigger caspases as a signalling mechanism resulting in binding to the cell surface, thus inducing apoptosis. The extrinsic pathway is mediated by members of the TNF family. This includes Fas which employs adapter (Fadd) proteins in the cytosolic death domain involving bound pro-caspases such as pro-caspase-8. The intrinsic pathway can be mediated by the release of mitochondrial cytochrome c due to increased levels of pro-apoptotic proteins such as Bax. The binding of cytochrome c triggers Apaf-1 activation permitting it to bind to pro-caspase-9 [26]. Once activated, caspase-9 and capsase-8 will trigger caspase-3 (effector protease). This is an oversimplification of the intricacies that take place within the cells.

FDG-mNPs and endocytosis

Research has shown that nanoparticles of about 25 nm can be easily engulfed via the clathrin-dependent endocytic pathway within 20 minutes [27] based on theoretical models. The FDG-mNPs used in this study were 10–20 nm in size; therefore, they should have been transported in via the clathrin-dependent endocytic pathway. However, our results show that only a small amount of FDG-mNPs used the clathrin-dependent endocytic pathway. The nanoparticles that were transported, however, did manage to significantly change the morphology of the NCI-H727 spheroids, as seen by the reduction in roundness to 0.70 and the SI to 0.50.

Our results suggest that FDG-mNPs may favor GLUT transporters as they are crosslinked with FDG. An alternative experiment to carry out would be to use a variety of GLUT receptors to find out which receptors the FDG-mNPs favor the most. GLUT receptors in cancer have been extensively studied and the experiment will either match the published literature or disprove it.

2D vs 3D culture

Standard 2D cell culture requires a flat surface for cells to adhere to. 2D cell cultures have homogenous growth due to an even amount of growth factors and nutrients found in the media. This makes 2D cell cultures one of the most commonly used platforms in the scientific field. However, in some instances, 2D cell culture will deviate from how the environment is *in vivo*. This is one reason that 2D cell culture is not adequate for drug screening or delivery. In 1970, Sutherland et al. proposed the idea of spheroids to investigate cancers [28] and recently, 3D cell culture has been gaining interest for drug screening and delivery. The most vital characteristic of 3D cell culture that makes it an attractive platform is its ability to mimic the native environment of in vivo cells.

Conclusions

FDG-mNP was demonstrated to have cytotoxic effects on NCI-H7272 and SY5Y cancer cells. Concentrations of 0.075 mg/mL, 0.15 mg/mL, and 0.3 mg/mL decreased mean cell viability of NCI-H727 cancer cells to 92.5%, 82.9%, and 75%, respectively. FDG-mNPs were shown to have detrimental effects on the

viability of SY5Y cells: a decrease of 5.7%, 18.6%, and 36.4% was found for SY5Y cells treated with 0.075 mg/mL, 0.15 mg/mL, and 0.3 mg/mL concentrations of FDG-mNPs, respectively. We therefore conclude that FDG-mNPs are promising in the development clinical applications for the destruction of cancer cells.

Acknowledgements

Dr. Omer Aras who one of the authors was partially supported through the NIH/NCI Cancer Support Grant P30 CA008748 and the manuscript approved by Internal Review Board.

Disclosure Statement

No potential conflict of interest was reported by the authors.

Orcid

Perihan Unak 0000-0002-5464-2987

Rumbidzai Cheryl Budiyo 0000-0003-0584-7553

Alex Horsnzky 0000-0003-0615-5807

Volkan Yasakci 0000-0002-4133-3886

Gillian Pearce 0000-0003-1428-2021

Steve Russell 0000-0002-5491-900X

Omer Aras 0000-0003-1758-0542

Oguz Akin 0000-0002-2041-6199

Julian Wong 0000-0002-9708-9077

References

[1]. Amin P., Patel M. *Asian Journal of Nanosciences and Materials,* 2020, **3**:24

[2]. Patra J.K., Das G., Fraceto L.F., Campos E., Rodriguez-Torres M., Acosta-Torres L.S., Diaz-Torres L.A., Grillo R., Swamy M.K., Sharma S., Habtemariam S., Shin H.S. *Journal of Nanobiotechnology*, 2018, **16**:71

[3]. Poh S., Chelvam V., Low P.S. *Nanomedicine (Lond).*, 2015, **10**:1439

[4]. De Jong W.H., Borm, P.J. *International Journal of Nanomedicine*, 2008, **3**:133

[5]. Ma L., Kohli M., Smith A. *ACS Nano,* 2013, **7**:9518

[6]. Guo P., Liu D., Subramanyam K., Wang B., Yang J., Huang J., Auguste D.T., Moses M.A. *Nature Communications*, 2018, **9**:130

[7]. Subramanian M., Pearce G., Guldu O.K., Tekin V., Miaskowski A., Aras O., Unak P. *IEEE Transactions on NanoBioscience,* 2016, **15**:517

[8]. San-Millán I., Brooks G.A. *Carcinogenesis*, 2017, **38**:119

[9]. Park S.G., Lee J.H., Lee W.A., Han K.M. *Nuclear Medicine and Biollogy,* 2012, **39:**1167

[10]. Yasakci V., Tekin V., Guldu O.K., Evren V., Unak P. *Journal of Radioanalytical and Nuclear Chemistry,* 2018, **318**:1973

[11]. Oh N., Park J.H. *International Journal of Nanomedicine,* 2014, **9**:51

[12]. Ailenberg M., Di Ciano-Oliveira C., Szaszi K., Dan Q., Rozycki M., Kapus A., Rotstein O.D. *British Journal of Pharmacology*, 2015, **172**:3748

[13]. Edmondson R., Broglie J.J., Adcock A.F., Yang L. *Assay and Drug Development Technologies*, 2014, **12**:207

[14]. Ozkaya F., Unak P., Medine E.I., Sakarya S., Unak G., Timur S. *Journal of Radioanalytical and Nuclear Chemistry*, 2013, **295**:1789

[15]. Watkins A.J., Pearce G., Unak P., Guldu O.K., Yasakci V., Akin O., Aras O., Wong J., Ma, X. *Journal of Biomedical Nanotechnology*, 2018, **14**:1979

[16]. Aras O., Pearce G., Watkins A.J., Nurili F., Medine E.I., Guldu O.K., Tekin V., Wong J., Ma X., Ting R., Unak P. *PloS One*, 2018, **13**:e0202482

[17]. Schindelin J., Arganda-Carreras I., Frise E., Kaynig V., Longair M., Pietzsch T., Preibisch S., Rueden C., Saalfeld S., Schmid B., Tinevez J.Y.,

White D.J., Hartenstein V., Eliceiri K., Tomancak P., Cardona A. *Nature Methods,* 2012, **9**:676
[18]. Halkes K.M., Souza A.C., Maljaars E.P., Gerwig G.J., Kamerling J.P. *European Journal of Organic Chemistry*, 2005, **17**:3650
[19]. Schneider C.A., Rasband W.S., Eliceiri K.W. *Nature Methods,* 2012, **9**:671
[20]. Ivanov D.P., Parker T.L., Walker D.A., Alexander C., Ashford M.B., Gellert P.R., Garnett M.C. *PLoS One*, 2014, **9**:e103817
[21]. Amaral R.L.F., Miranda M., Marcato P.D., Swiech K. *Frontiers in Physiology*., 2017, **8**:605
[22]. Kelm J.M., Timmins N.E., Brown C.J., Fussenegger M., Nielsen L.K. *Biotechnology and Bioengineering*, 2003, **83**:173
[23]. Zanoni M., Piccinini F., Arienti C., Zamagni A., Santi S., Polico R., Bevilacqua A., Tesei A. *Scientific Reports*, 2016, **6**:19103
[24]. Roa W., Xiong Y., Chen J., Yang X., Song K., Yang X., Kong B., Wilson J., Xing J.Z. *Nanotechnology*, 2012, **23**:375101
[25]. Hu C., Niestroj M., Yuan D., Chang S., Chen J. *International Journal of Nanomedicine*, 2015, **10**:2065
[26]. Haraguchi M., Torii S., Matsuzawa Si., Xie Z., Kitada S., Krajewski S., Yoshida H., Mak T.W., Reed J.C. *Journal of Experimental Medicine.,* 2000, **191**:1709
[27]. Gao H., Shi W., Freund L. B., *Proceedings of the National Academy of Sciences*, 2005, **102**:9469
[28]. Sutherland R.M., McCredie J.A., Inch W.R. *Journal of the National Cancer Institute*, 1971, **46**:113

How to cite this manuscript: Perihan Unak*, Rumbidzai Cheryl Budiyo, Alex Horsnzky, Volkan Yasakci, Gillian Pearce, Steve Russell, Omer Aras, Oguz Akin, Julian Wong. Effects of fluorodeoxyglucose magnetic nanoparticles on NCI-H727 and SH-SY5Y cancer cells. *Asian Journal of Nanoscience and Materials*, 4(1) 2021, 53-66. DOI: 10.26655/AJNANOMAT.2021.1.5